

The Vibrational Properties of Ultrananocrystalline Diamond Based on Molecular dynamics Simulations

Shashishekar P. Adiga¹, Vivekananda P. Adiga², Robert W. Carpick³ and Donald W. Brenner⁴

¹Kodak Research Laboratories, Eastman Kodak Company, Rochester, NY 14650, U.S.A.

²School of Applied and Engineering Physics, Cornell University, Ithaca, NY 14853, U.S.A.

³Department of Mechanical Engineering and Applied Mechanics, University of Pennsylvania, Philadelphia, PA 19104, U.S.A.

⁴Department of Materials Science and Engineering, North Carolina State University, Raleigh, NC 27695, U.S.A.

ABSTRACT

We investigate the vibrational properties of ultrananocrystalline diamond (UNCD) using molecular dynamics simulations. We compare the vibrational spectra of two UNCD models of average grain size 2 and 4 nm with single crystal diamond and an isolated nanodiamond (ND) particle. The vibrational spectra of the ND particle and UNCD models exhibit the effect of phonon confinement as well as undercoordinated atoms at the surface/interfaces. This is further reflected in the specific heat of UNCD models and the ND particle that showed enhancements over that of single crystal diamond. The excess specific heat in UNCD models in comparison to single crystal diamond is found to be maximum at approximately 350 K.

INTRODUCTION

The superlative properties of diamond in terms of stiffness and high thermal and chemical stability have made it attractive for use in microelectromechanical systems (MEMS) and there is a growing interest in diamond thin films grown by chemical vapor deposition. UNCD is microwave plasma or hot filament CVD grown polycrystalline diamond with grain sizes in the range of 2–5 nm. UNCD films have distinct advantages over conventional microcrystalline diamond films because conformal UNCD thin films exhibit smooth surfaces as compared to microcrystalline diamond films, and can be grown at complementary metal oxide semiconductor (CMOS) compatible temperatures (~ 400 °C) [1]. Additionally, physical properties, such as Young's modulus, hardness, and acoustic velocity remain close to single-crystal diamond despite the high volume fraction of grain boundaries and the presence of atoms such as hydrogen [2]. It is important to analyze the vibrational spectra of UNCD as nanocrystalline materials, due to a considerable fraction of grain boundary atoms, differ from the vibrational properties of materials composed of larger grain sizes. Vibrational properties directly influence several material properties including, for example, the specific heat capacity, the thermal expansion coefficient, the thermal conductivity (specifically at low temperatures), and the temperature dependence of the elastic constants [3]. Hence, to gain a detailed understanding of vibrational properties we have performed molecular dynamics simulations of nanodiamond materials. In particular, we will compare vibrational power spectra and specific heat for bulk diamond, two UNCD models of 2 and 4 nm grain sizes, and a 4 nm cuboctahedral nanodiamond particle.

COMPUTATIONAL DETAILS

The force field we have used in these simulations is the second-generation reactive empirical bond order (REBO-II) potential [4]. This potential function successfully models both sp^2 and sp^3 bonding, depending on local coordination and the degree of conjugation. Classical equations of motion for each atom were numerically integrated using a third-order Nordsieck predictor-corrector algorithm with a time step size 0.5 fs. Prior to calculating the properties, the system was equilibrated at a given temperature using a Langevin thermostat. The NVE ensemble was used for production runs.

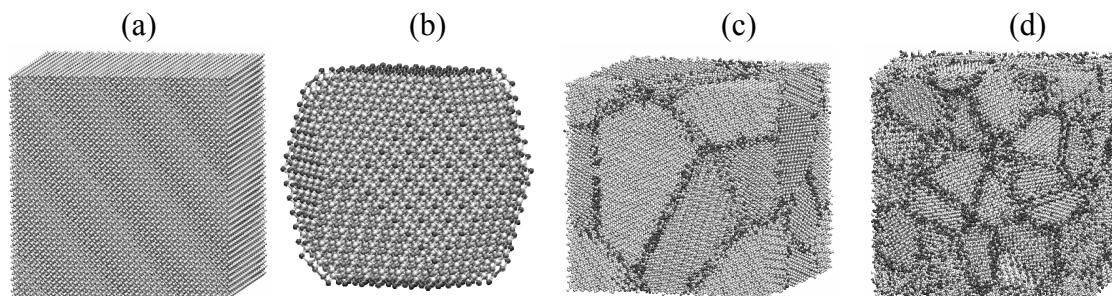


Figure 1. The model systems used in this work: (a) single crystal diamond (b) 4 nm cuboctahedral nanodiamond (ND); (c) UNCD (4 nm) (d) UNCD (2 nm). Under-coordinated atoms are colored dark to indicate the grain boundaries

Table 1. Properties of the Model Systems Simulated.

	Diamond	ND	UNCD (4 nm)	UNCD (2nm)
number of atoms	64000	6232	82696	81769
number of grains/particles	-	1	8	66
sp^1 content (%)	0	8.2	.9	4
sp^2 content (%)	0	6.7	11.6	23.7
sp^3 content (%)	100	85.1	87.5	72.3
box dimension (Å)	70.89	-	78.56	80.51

The model systems considered in this study are illustrated in Figure 1. The UNCD (4 nm) and UNCD (2 nm) are 3-D periodic models of UNCD of average 4 nm and 2 nm grain sizes, respectively. We used a Voronoi construction to build UNCD models as detailed in our earlier work [5]. Before performing production runs, we annealed the UNCD systems for 50 ps at 1000 K, allowing unfavorable configurations in the grain boundaries to relax. The single crystal diamond model used in this study consisted of a 3-D periodic cell with $b = 70.89$ Å, with 64,000 C atoms in the diamond lattice. The ND particle is of cuboctahedral (CO) shape and consisted of 6232 atoms. The CO particle consists of eight $\{111\}$ and six $\{100\}$ facets. The model was cut out from an ideal diamond crystal with the lattice constant 3.56 Å. Each of these facets is at

approximately 40 Å from the center of the cluster. The key properties of the four model systems studied are tabulated in Table 1.

The specific heat within the harmonic approximation was calculated by first determining the normalized power spectrum, $g(\nu)$, where ν is the vibrational mode frequency. The power spectrum was determined by Fourier transforming the velocity autocorrelation function (VACF) obtained from the simulations and then normalizing such that $\int g(\nu)d\nu = 1$. To calculate the VACF, the velocities of all atoms were sampled every 2 fs time step for 2.5 ps.

RESULTS AND DISCUSSION

Vibrational Spectra

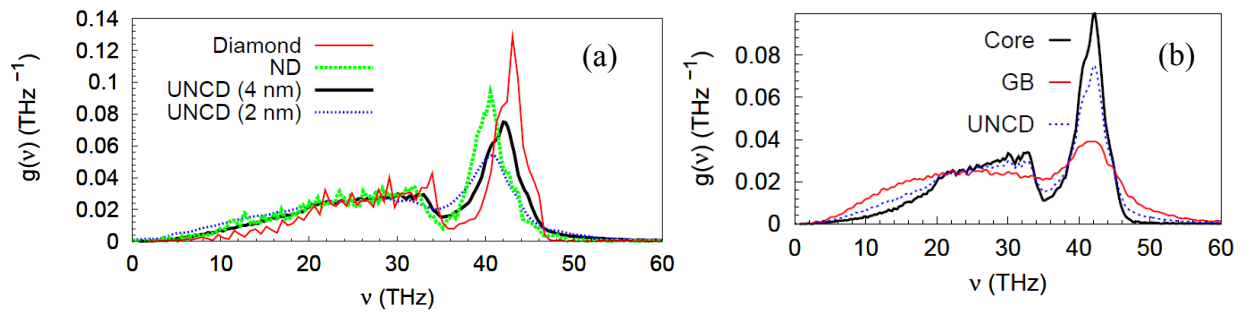


Figure 2. (a) The calculated vibrational spectra of UNCD (4 nm), UNCD (2 nm), ND particle, and single crystal diamond (solid line) at $T = 300\text{K}$. (b) The partial spectra due to grain boundary and core atoms for the UNCD (4 nm) system at $T = 300\text{K}$.

In Figure 2 (a), we have plotted the computed vibrational spectra at $T = 300\text{K}$ for the two UNCD model systems, the ND particle and the single crystal diamond. Before comparing the spectra of the model systems, it is important to point out that simulated vibrational spectra have, in general, features shifted to higher energies compared to experiment. This shift lies within the range of deviations observed in previous calculations using bond-order potentials [8]. Nonetheless, the calculated power spectrum bears reasonably good agreement with the experimental vibrational spectrum of diamond [9]. The main feature of the spectrum for single crystal diamond is a strong peak at $\sim 43.2\text{ THz}$ (1425 cm^{-1}) with two shoulders around 41.5 (1384 cm^{-1}) and 45 (1501 cm^{-1}) THz. This peak is followed by a smaller peak at 33.7 THz (1128 cm^{-1}) and a relatively flat region at intermediate frequencies. The overall features of the vibrational spectra of UNCD systems and the ND particle system are similar to that of single crystal diamond. However, there are significant differences, most notably, the whole spectrum in each nanodiamond model is red shifted in comparison to diamond. For example, in the case of UNCD (4 nm) the main peak around 43 THz is red-shifted to 42 THz, an effect of phonon confinement which is common to nanocrystalline materials. Also, this peak is broader and smaller for UNCD. The red shift for the UNCD (2 nm) system is larger owing to smaller crystallite size. The ND particle exhibits the largest shift in the spectrum as it has free surfaces in addition to the phonon confinement effect. For UNCD systems and the ND particle, a high-frequency tail extends beyond 47 THz. The high-frequency tail is attributed to strained bonds involving under-coordinated atoms in the grain boundaries/surfaces that have enhanced force constants.

In Figure 2 (b) we show normalized partial spectra of grain boundary (GB) and core atoms for the UNCD (4 nm) system at 300 K. The GB atoms are defined as all the undercoordinated atoms (sp^2 and sp^1 hybridized) and atoms that are within a distance of 3 Å from them. The remaining atoms are defined as core (interior) atoms. For comparison the total spectrum of the UNCD (4 nm) system is also plotted. The spectrum of GB atoms is clearly disordered as it shows signatures of both under-coordinated and sp^3 atoms. The optical peak due to sp^3 atoms in the core region is red-shifted to 42 THz as compared to single crystalline diamond (43.2 THz) due to the phonon confinement effect. Based on the comparison of the spectra of GB and core atoms with the total spectra of the UNCD system, the enhancement of the acoustical modes at lower frequency can be directly attributed to the GB atoms.

Specific heat and Debye temperature

To study the effect of temperature on the specific heat of UNCD, the phonon specific heats of UNCD and diamond are computed from the temperature dependent vibrational spectra using the following equation.

$$C_V = \frac{h^2}{k_B T^2} \int_0^\infty \frac{\nu^2 \exp(h\nu/k_B T)}{(\exp(h\nu/k_B T) - 1)^2} g(\nu) d\nu \quad (1)$$

The plot in Figure 3 shows the specific heat of UNCD (4 nm), UNCD (2 nm), ND particle and single crystal diamond as a function of temperature. We note that our computed value C_V of diamond is lower than that of experimental values, for example, the computed C_V is 380 J/Kg-K at 300 K as compared to the experimental value of 502 J/Kg-K. This discrepancy is due to many factors including (i) the absence of defects such as vacancies, impurities and isotopes in our model and (ii) the interatomic potential. For example, previous calculations [10] of C_V of diamond employing the REBO-II have reported similar deviations in the computed C_V from experimental values.

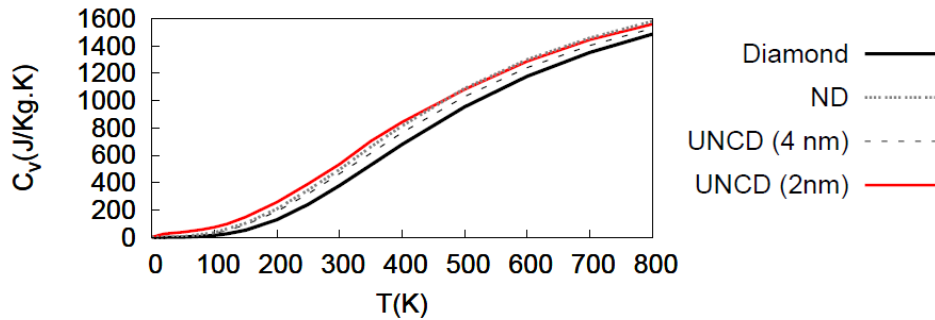


Figure 3. Temperature dependence of (a) the specific heat at constant volume for UNCD (4 nm), UNCD (2 nm), ND particle and diamond systems.

The specific heat of all three nanodiamond models are enhanced as compared to single crystal diamond over the whole range of the temperature we have considered. The excess specific heat as a function of temperature is plotted in Figure 4. For comparison, the excess specific heat of graphite compared against diamond as obtained from ref. [6] is also plotted. The excess specific heat of UNCD systems go through a maximum value at approximately 350 K and the C_V values for UNCD (4 nm) and UNCD (2 nm) models are 15 % and 33 % greater, respectively, than single crystal diamond.

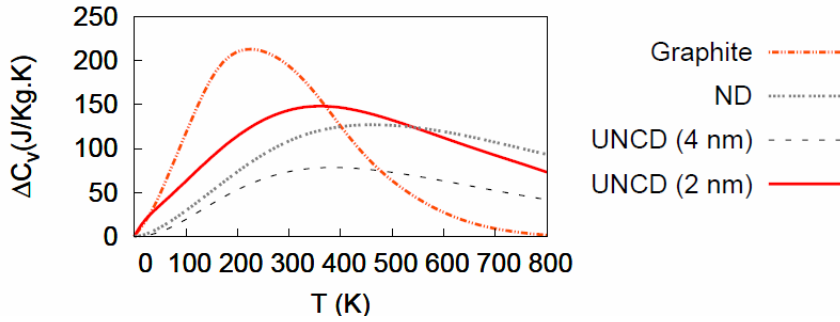


Figure 4. The excess specific heat of UNCD models and ND particle as compared to single crystal diamond. For comparison, the excess specific heat for graphite as reported in ref. [6] is also plotted.

The relative importance of contributions from frequencies < 20 THz occurs mostly at low temperatures. As the temperature increases the relative contribution of excess states in the low to medium frequency region in UNCD becomes less important. Therefore, the excess C_v goes through a maximum around 350 K. In comparison, the maximal excess for bulk graphite in relation to bulk single crystal diamond (Figure 4) occurs around 200 K. Note that in UNCD excess specific heat is due to the contributions from atoms at grain boundaries (under-coordinated sp^2 and sp^1 atoms, sp^3 atoms bonded to under-coordinated atoms, or sp^3 atoms very close to grain boundaries) which have slightly different bonding energies as opposed to the perfect order of sp^3 bonded diamond or sp^2 bonded graphite. We note that the sharp sp^3 features of single crystal diamond or sp^2 bonded graphite visible in the VDOS are broadened by the different energy landscapes due to the disorder at the grain boundaries. This broadening of the VDOS features results in excess specific heat.

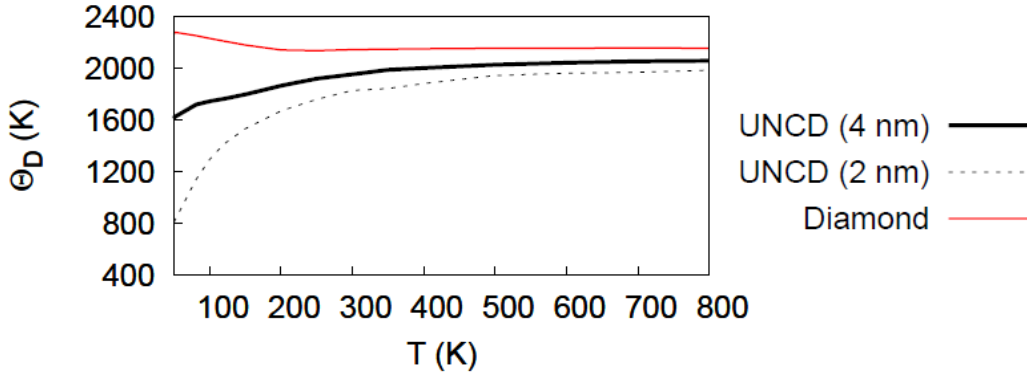


Figure 5. The Debye temperature as a function of temperature for UNCD (4 nm) and UNCD (2 nm) models and diamond.

We now turn to the Debye temperature of UNCD. It is proportional to the Debye frequency and within the harmonic approximation relates to the stiffness of the material. From the simulated C_v vs temperature behavior we calculate the Debye temperature as a function of temperature as detailed elsewhere [5, 7]. We plotted the Debye temperatures for the two UNCD systems and diamond models as a function of temperature in Figure 5. The Debye temperature of diamond is overestimated in our calculations [6] because the simulated C_v values in our work is

lower than the experimental values as discussed previously. However, the relative values of diamond and UNCD models can provide important information about the stiffness of the material. The Debye temperatures of UNCD (2 nm) and UNCD (4 nm) systems are approximately 15 % and 9% lower, respectively, than that of diamond at 300 K. The softening of UNCD can be explained on the basis of grain boundary atoms leading to an enhancement of soft modes in the vibrational spectra as compared to diamond.

CONCLUSIONS

Our analysis of the vibrational properties of UNCD leads us to conclude that the vibrational density of states exhibit enhancements that arise from atoms at and near the grain boundaries. This is reflected in the calculated phonon specific heat of UNCD, which is enhanced as compared to single crystal diamond. Because these enhancements are in the 5-20 THz frequency region, the excess C_v as a function of temperature goes through a maximum value at approximately 350 K, above which the low to medium frequency enhancements contribute less and less to specific heat. In addition, the Debye temperature of UNCD reflects reduced stiffness which is more severe for a smaller grain size.

ACKNOWLEDGMENTS

Use of computer resources from the Computational Center for Nanotechnology Innovations (CCNI) at Rensselaer Polytechnic Institute (RPI) is gratefully acknowledged. VPA and RWC are supported by the Nano/Bio Interface Center through the National Science Foundation NSEC (DMR08-32802). DWB is supported by the Office of Naval Research through contract N000141-01-01-6-8.

REFERENCES

1. A. R. Krauss, O. Auciello, D. M. Gruen, A. Jayatissa, A. Sumant, J. Tucek, D. C. Mancini, N. Moldovan, A. Erdemir, and D. Ersoy, *Diamond Relat. Mater.*, **10**, 1952, (2001).
2. D. M. Gruen, *Ann.Rev. Mat. Sci.* **29**, 211 (1999).
3. V. P. Adiga, A. Datta, S. Suresh, J. A. Carlisle, and R. W. Carpick, submitted to *J. App. Phys.*
4. D. W. Brenner, O. A. Shenderova, J. A. Harrison, S. J. Stuart, B. Ni, and S. B. Sinnott, *J. Phys.: Cond. Matt.* **14**, 783 (2002).
5. S. P. Adiga, V. P. Adiga, R. W. Carpick and D. W. Brenner, *J. Phys. Chem. C*, **115**, 21691 (2011).
6. N. Mounet and N. Marzari, *Phys. Rev. B.* **71**, 205214 (2005).
7. T. Tohei, A. Kuwabara, F. Oba, and I. Tanaka, *Phys. Rev. B*, **73**, 064304 (2006).
8. I. Rosenblum, J. Adler and S. Brandon, *Comp. Mat. Sci.* **12**, 9 (1998).
9. J. Walker, *Rep. Prog. Phys.* **42**, 1605 (1987).
10. H. Jiang, Y. Huang, K. C. Hwang, *J. Eng. Mat. Tech.* **127**, 408 (2005).